6ICEGE
6th International Conference on Earthquake Geotechnical Engineering
1-4 November 2015
Christchurch. New Zealand

Effect of Material Inhomogeneity on Liquefaction Behavior of Natural Deposits by Effective Stress Analysis

R. Uzuoka[1], N. Yoshida[2], N. Kawasaki[3] and H. Ishikawa[4]

ABSTRACT

This study discussed the effect of modeling methods for liquefiable soil layers on the liquefaction behavior during and after an earthquake. We carried out effective stress analysis with the soil data at Kawauchi town in Tokushima. For the liquefiable alluvial layer, we examined the differences between conventional layer based modeling using the representative material parameters set, and element based modeling using the multi material parameter sets at every one meter depth. The numerical results showed that liquefaction and subsequent subsidence occurred in both cases, however the dissipation of excess pore water pressure and convergence of subsidence were different each other. There are cases that conventional layer based modeling becomes too conservative.

Introduction

The Great East Japan Earthquake in 2011 caused extensive liquefaction throughout reclaimed lands and man-made islands in Kanto region, which caused serious damage to a lot of houses and infrastructures (Yasuda et al. 2012). There is concern that wide range of liquefaction occurs at the mouth delta of the Yoshino River in Tokushima, Japan, which has loose Holocene deposits near the surface part when the Nankai trough earthquake occurs in the future.

Effective stress analyses have been widely used for liquefaction assessments of various structures. In conventional liquefaction analyses each soil layer was modeled with a homogeneous layer with the same material constants. The material parameters of constitutive models were determined to reproduce the mechanical properties obtained by laboratory tests with undisturbed soil samples such as undrained cyclic shear tests. In Japan most popular test for. liquefaction strength is so called liquefaction test to obtain a relationship between cyclic shear stress ratios and numbers of cycles for a certain strain level. The liquefaction test needs at least three undisturbed samples with high quality. It is sometimes difficult to get homogeneous samples to represent the properties of target soil layer; it needs engineering sense to get the representative samples for a thick inhomogeneous soil layer. Meanwhile in-situ sounding tests such as CPT/SPT can get continuous/every one meter data along thick soil layer although the mechanical properties cannot be directly obtained. The mechanical properties can be estimated by empirical models; however the applicability should be carefully examined in effective stress analyses.

[1]Professor, Dept. of Civil Engineering, Tokushima University, Tokushima, Japan, uzuoka@tokushima-u.ac.jp
[2]Graduate Student, Dept. of Civil Engineering, Tokushima University, Tokushima, Japan
[3]Graduate Student, Dept. of Civil Engineering, Tokushima University, Tokushima, Japan
[4]Consulting Engineer, Geotechnical and Environmental Engineering Div., NIPPON KOEI Co., Ltd., Tokyo, Japan

This study discussed the effect of vertical modeling methods for liquefiable soil layers on the liquefaction behavior during and after an earthquake. As the numerical examples we performed effective stress analyses with the soil properties of the Tokushima plain deposits. In the effective stress analyses, we used conventional layer based modeling method in which the material parameters were the same in each liquefiable soil layer, and element based modeling method in which the material parameters were different at every one-meter depth as shown in Figure 1. In the conventional layer based modeling the material parameters can be determined from laboratory tests with undisturbed samples such as cyclic undrained triaxial tests, while the material parameters can be determined from empirical models with physical properties and in-situ tests in the element based modeling. Therefore the element based modeling can consider vertical inhomogeneous material properties in the same soil layer although the material parameters cannot directly determined from the laboratory tests. Although horizontal inhomogeneity should be considered in liquefaction analyses, this study focused on vertical inhomogeneity only.

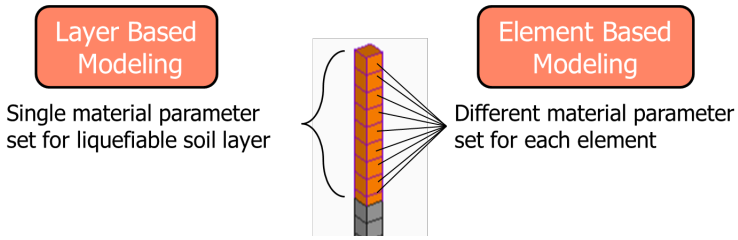

Figure 1: Modeling of liquefiable layer.

Effective Stress Method

Effective stress method, program code LIQCA, uses *u-p* formulation (Oka et al. 1994). Finite element method (FEM) is used for spatial discretization of the equilibrium equation, whereas the finite volume method is used for spatial discretization of the pore water pressure in the continuity equation. The Newmark implicit method is used for time integration. The governing equations are formulated using the following assumptions: 1) infinitesimal strain, 2) smooth distribution of porosity in the soil, 3) small acceleration of the fluid phase relative to that of the solid phase com-pared with the acceleration of the solid phase, and 4) incompressible grain particles in the soil. The equilibrium equation for the mixture is derived as

$$\rho\ddot{\mathbf{u}}^{\mathrm{S}} - \mathrm{div}\boldsymbol{\sigma} - \rho\mathbf{b} = \mathbf{0} \tag{1}$$

where ρ: overall density, $\mathbf{u}^{\mathrm{S}}$: displacement vector of the solid, $\boldsymbol{\sigma}$: total stress tensor, and $\mathbf{b}$: body force vector. The continuity equation is derived as:

$$\frac{n}{K^{\mathrm{F}}}\dot{p} + \dot{\varepsilon}_{\mathrm{v}}^{\mathrm{S}} + \mathrm{div}\left\{\frac{k}{\rho^{\mathrm{F}}g}\left(-\mathrm{grad}\,p + \rho^{\mathrm{F}}\mathbf{b} - \rho^{\mathrm{F}}\ddot{\mathbf{u}}^{\mathrm{S}}\right)\right\} = 0 \tag{2}$$

where n: porosity, K^{F}: bulk modulus of the fluid, $\varepsilon^{\mathrm{S}}{}_{\mathrm{v}}$: volumetric strain of the solid, k: coefficient

of permeability, ρ^F: real fluid density, g: gravity acceleration and p: pore water pressure. Extensive stress, extensive strain, and compressive pore water pressure are defined as positive. The constitutive equation used for sand is a cyclic elasto-plastic model (Oka et al. 1999). The constitutive equation is formulated using the following assumptions: 1) the infinitesimal strain, 2) the elasto-plastic theory, 3) the non-associated flow rule, 4) the concept of the overconsolidated boundary surface, and 5) the nonlinear kinematic hardening rule. The numerical method with this constitutive model has been validated in various liquefaction problems (Uzuoka et al. 2007, Uzuoka et al. 2008).

Numerical Conditions

This investigation site is Kawauchi area in Tokushima city where is a delta area of the downstream basin of Yoshino river. Figure 2 shows the soil profile of the investigation site. The surface soil layers F2g and F1g are filled layer above the ground water table. The soil layer A2s mainly composed of Holocene sandy loose deposits with the thickness of about 10 meters where the liquefaction potential is extremely high. The deeper soil profiles consist of Holocene transgression clay and sand, and Pleistocene gravel which is the base layer for earthquake motions. We applied cyclic elasto-plastic model for the sandy layer A2s that has a high potential of liquefaction and Ramberg-Osgood model (R-O model) for other layers that are less likely to liquefy. As mentioned above, we performed two numerical cases with conventional layer based modeling and element based modeling of liquefiable layers.

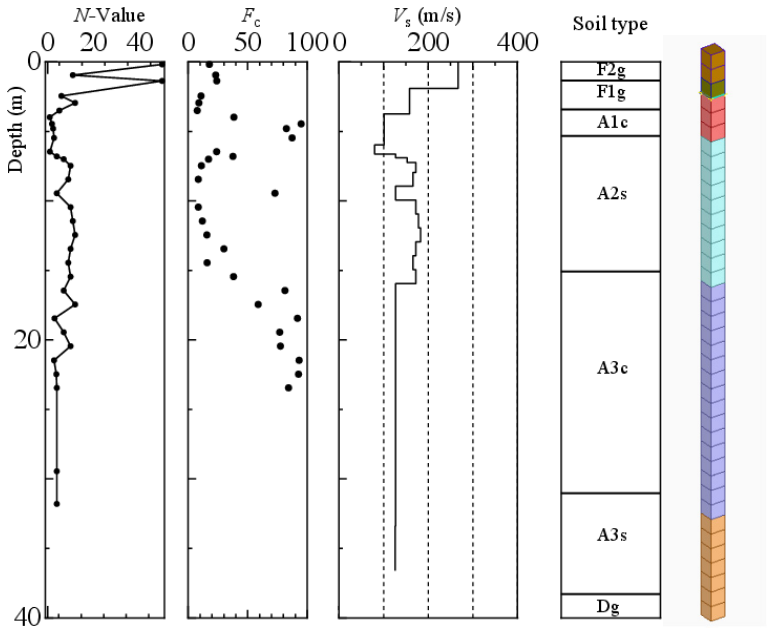

Figure 2: Soil profile and the finite element model.

Common numerical conditions

The finite element model of the investigation site is also shown in Figure 2. We used the three dimensional soil column in order to consider both horizontal seismic motions, and the height of each element was about one meter. As the initial conditions we used the initial effective stress

calculated by coefficient of earth pressure at rest of 0.5 and effective overburden pressure. We set viscous boundary at the upper surface of Dg layer, and tied displacements of nodes at the same depth along the lateral boundaries. The upper surface of A2s was drainage and others boundaries were non-drainage for the pore water. We used strong-motion acceleration waveforms (Cabinet Office 2012) as the input motions shown in Figure 3. The material parameters of R-O model for F2g, F1g, A1c, A3c and A3s layers were identical in both cases. They were determined from strain dependencies of shear modulus and damping factor obtained by empirical models. The time increment of calculation was 0.002 seconds, and the coefficients of Newmark time integration methods were 0.3025 and 0.6. The Rayleigh damping proportional to the initial stiffness was used to ensure the numerical stability, and the coefficient was 0.003.

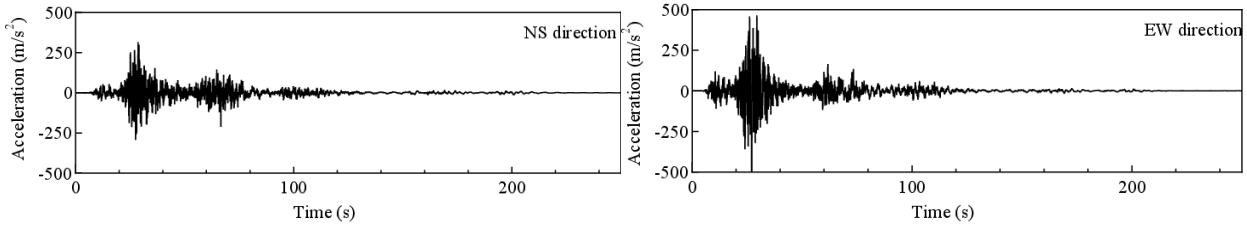

Figure 3: Input acceleration at Dg layer (Cabinet Office 2012).

Layer based modeling of liquefiable layer

"LBM" column in Table 1 shows the material parameters for A2s layer with the layer based modeling (LBM). In this case we used a single parameter set for A2s layer. We set the material parameters of the elasto-plastic model for A2s layer as follows. We directly set the initial void ratio e_0, the initial shear modulus G_0 from PS-logging, and the failure stress ratio M_f from monotonic drained triaxial tests. The hydraulic conductivity k was empirically estimated from particle size D_{20}. The remaining parameters were adjusted to reproduce the liquefaction behavior such as the liquefaction strength and development of pore water pressure and shear strain during cyclic shear obtained by cyclic undrained triaxial tests with undisturbed soil samples. Figure 4 shows the liquefaction strength curves and time histories of pore water pressures for laboratory tests and simulations.

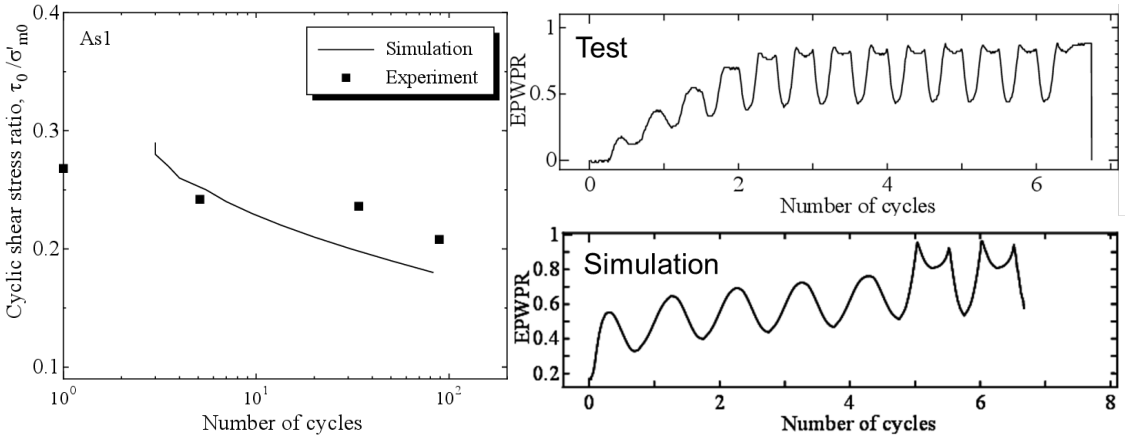

Figure 4: Liquefaction strength and pore water pressure of A2s layer.

Table 1. Material parameters for A2s layer in both modeling

	LBM	EBM	EBM	EBM	EBM	EBM	EBM	EBM	EBM	EBM	EBM
Layer/Sample	A2s	1-S-1	P-11	P-12	P-13	P-14	P-15	P-16	P-17	P-18	P-19
Depth (m)	-	6.80	7.47	8.45	9.45	10.45	11.45	12.45	13.45	14.45	15.45
N-Value	-	4	10	9	4	10	11	12	10	9	10
Fc (%)	-	37.6	11.1	8.5	72.9	8.5	11.9	15.7	30.0	15.9	38.1
RL20	0.242	0.196	0.224	0.203	0.247	0.201	0.211	0.224	0.237	0.192	0.242
Density (g/cmm3)	2.08	1.97	1.99	2.03	2.27	2.01	2.03	2.07	2.00	2.36	2.17
Initial void ratio	0.694	0.728	0.694	0.694	0.694	0.694	0.694	0.694	0.694	0.694	0.694
Permeability cefficient (m/s)	2.25E-05	2.25E-05	2.25E-05	2.25E-05	2.25E-05	2.25E-05	2.25E-05	2.25E-05	2.25E-05	2.25E-05	2.25E-05
Vs (m/s)	169	127	172	166	127	172	178	183	172	166	172
Normalized shear modulus	486.9	381.4	660.2	564.5	327.3	489.8	486.1	487.2	390.3	394.4	363.2
Poisson's ratio	0.25	0.25	0.25	0.25	0.25	0.25	0.25	0.25	0.25	0.25	0.25
Compression index	0.01250	0.00700	0.00710	0.00560	0.02010	0.00640	0.00780	0.00990	0.01520	0.00600	0.01740
Swelling index	0.00125	0.00070	0.00071	0.00056	0.00201	0.00064	0.00078	0.00099	0.00152	0.00060	0.00174
Failure stress ratio	1.020	1.260	1.260	1.260	1.260	1.260	1.260	1.260	1.260	1.260	1.260
Phase transformation stress ratio	0.909	0.909	0.909	0.909	0.909	0.909	0.909	0.909	0.909	0.909	0.909
Hardening parameter	2397.7	817.3	1938.8	1299.2	1480.7	1166.2	1234.6	1469.3	1486.7	814.0	1527.8
Hardening parameter	48.0	16.3	38.8	26.0	29.6	23.3	24.7	29.4	29.7	16.3	30.6
Dilatancy parameter	2.0	1.0	1.0	1.0	1.0	1.0	1.0	1.0	1.0	1.0	1.0
Dilatancy parameter	8.0	5.0	5.0	5.0	5.0	5.0	5.0	5.0	5.0	5.0	5.0
Reference strain parameter	0.0130	0.0500	0.0147	0.0222	0.0162	0.0222	0.0250	0.0208	0.0179	0.0500	0.0121
Reference strain parameter	0.0180	0.0400	0.0200	0.0200	0.0350	0.0200	0.0300	0.0250	0.0250	0.0300	0.0300

Element based modeling of liquefiable layer

"EBM" columns in Table 1 shows the material parameters for A2s layer with the element based modeling (EBM). In this case we used different parameter sets for each element in A2s layer, and the other layers have the same parameters as those in LBM case. We set the material parameters of the elasto-plastic model for A2s layer as follows. We used the same parameters for the hydraulic conductivity and the phase transformation stress ratio as those in LBM case. The initial void ratio and the failure stress ratio were determined empirically from representative existing data of A2s layer. The shear wave velocity was calculated by empirical equations with SPT N-values (JRA 2012). The remaining parameters were adjusted to reproduce the liquefaction behavior such as the liquefaction strength and strain development during cyclic shear. We computed the cyclic shear stress ratio for twenty cycles by means of empirical formula (JRA 2012) with N-value and fine content at every one meter depth in Table 1. Figure 5 shows the depth distributions of liquefaction strength with laboratory tests and empirical equations. Liquefaction strength with empirical equation roughly agree with those with laboratory tests with undisturbed samples. With regard to properties of strain development during cyclic shear, we used empirical models (Mikami et al. 2012) of liquefiable sandy layers in the Tokushima plane (Ishikawa et al. 2013). The models were bilinear relationships between the strain double amplitude DA and the number of cycles N_c for different range of fine contents with Fc < 35% and Fc > 35%. Figure 6 illustrates a typical result of $DA-N_c$ relations of sample 1-S-1 for the empirical model and the simulation by the cyclic elasto-plastic model. Although there was room for improvement about the first part of the $DA-N_c$ relations before initial liquefaction, the both slopes in the latter part approximately coincided with each other.

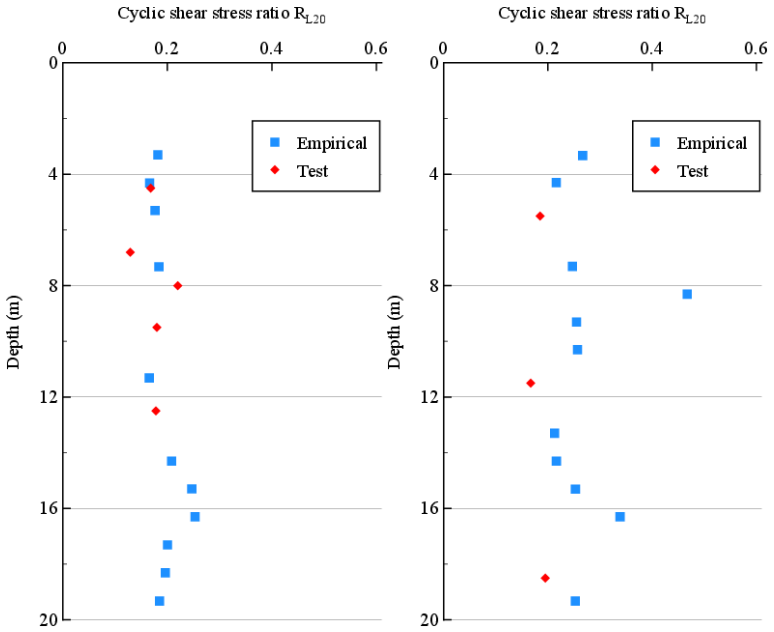

Figure 5: Distributions of liquefaction strength with tests and empirical equations.

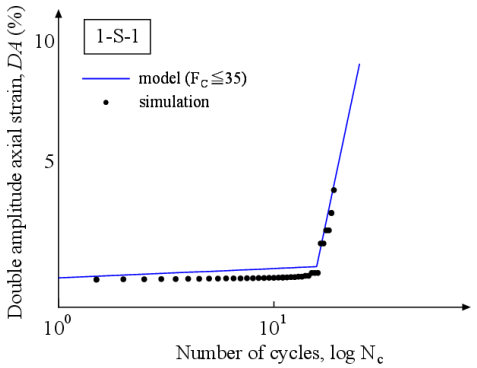

Figure 6: Strain development model of sample 1-S-1.

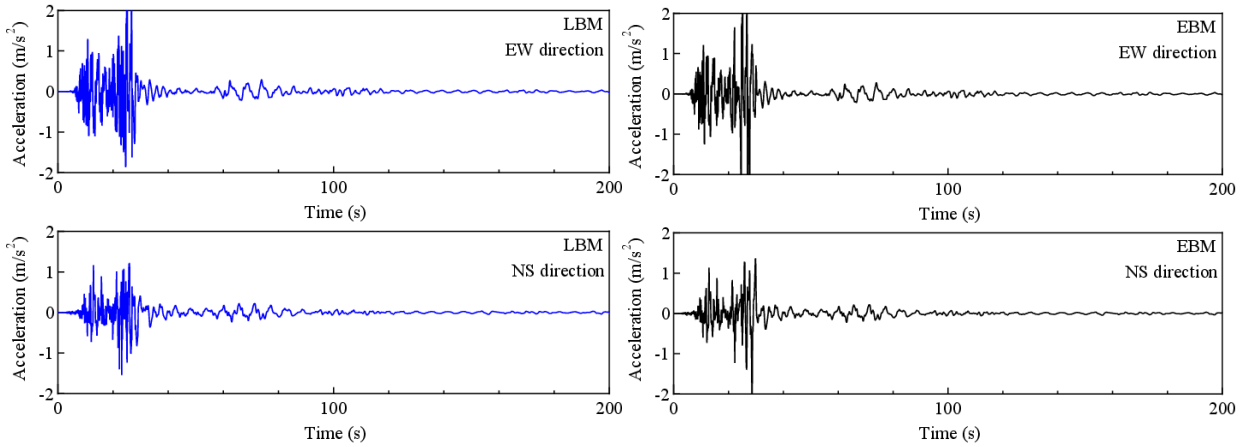

Figure 7: Horizontal acceleration responses at ground surface.

Numerical Results and Discussion

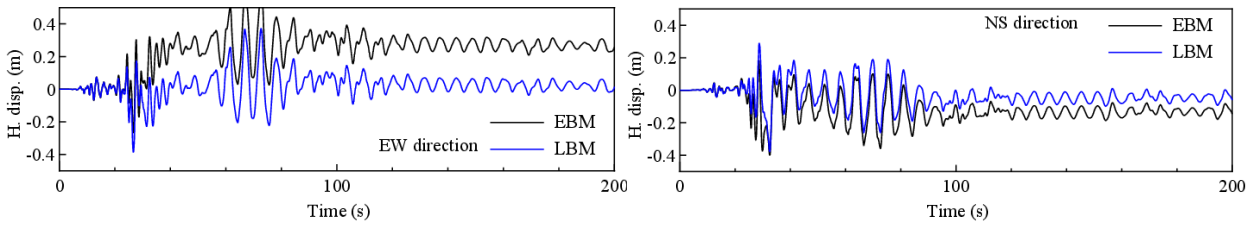

Figure 8: Horizontal displacement responses at ground surface.

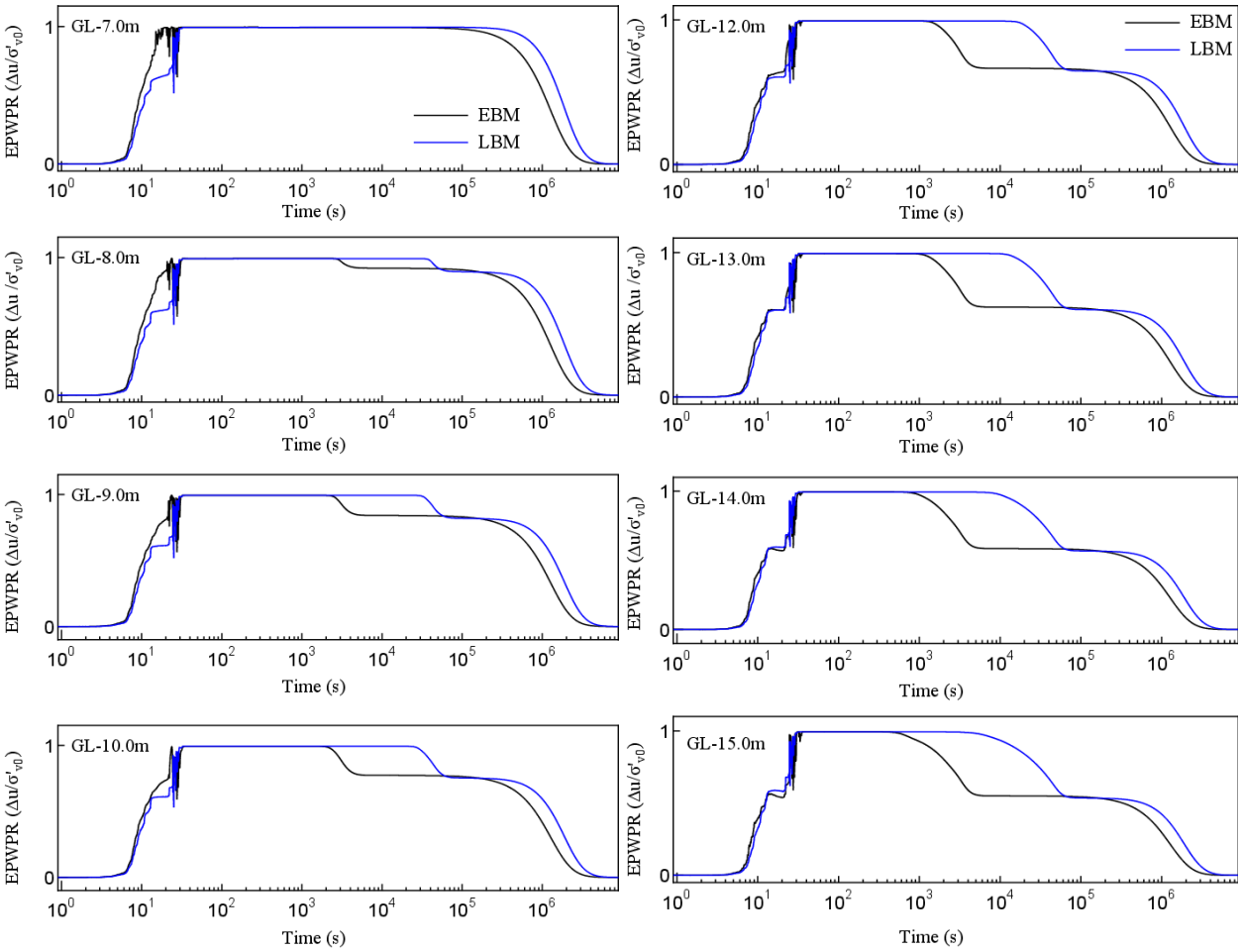

Figure 9: Excess pore water pressure ratios in A2s layer.

Figure 7 and 8 show the time histories of acceleration and displacement in both horizontal directions at ground surface for LBM and EBM cases. Figure 9 shows the time histories of excess pore water pressure ratio at each element in A2s layer. The excess pore water pressure ratio is the ratio of excess pore water pressure for initial effective overburden pressure. At any depth in A2s layer, liquefaction occurred at about 20 seconds, and this caused that the ground surface acceleration shown in Figure 7 attenuated after about 20 seconds. The generation process

of excess pore water pressure ratio in both cases were different from each other. At all elements the excess pore water pressure in EBM case dissipated earlier than LBM case. Figure 10 shows the time histories of vertical displacement at ground surface for both cases. The subsidence converged after about 17 hours in LBM case and about 11 hours in EBM case. In LBM case the amount of subsidence reached about 50 cm, while in EBM case the convergence of subsidence occurred earlier than case 1, and the amount of subsidence was suppressed about 30 cm. These differences between both cases are mainly due to the differences in the liquefaction strengths. The RL20 obtained by cyclic undrained shear tests in LBM case as shown in Figure 4 is almost the minimum value in those obtained by empirical model in EBM case shown in Table 1.

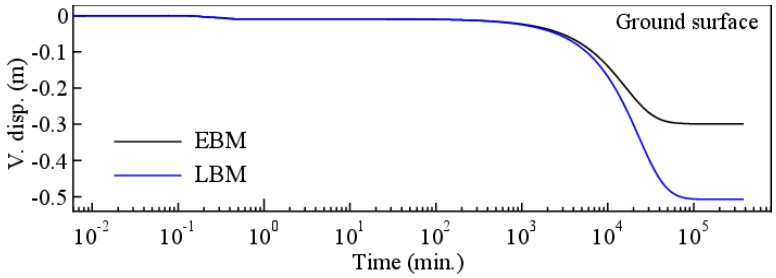

Figure 10: Vertical displacement responses at ground surface.

Conclusions

In this study, we carried out effective stress analyses with the soil data at Kawauchi area in Tokushima. For the liquefiable layer, we examined the differences between the conventional layer based modeling using the representative material parameters set, and the element based modeling using the multi material parameter sets at every one meter depth. With respect to the method for setting the material parameters in the element based modeling, we used empirical models for liquefaction strength and strain development during cyclic shear.

The numerical results showed that liquefaction and subsequent subsidence occurred in both cases, however the dissipation of excess pore water pressure and the subsidence were different in each modeling method. The inhomogeneity in the material parameters caused these differences. There are cases that the conventional layer based modeling becomes too conservative. We need further investigation to validate the both modeling method. The element based modeling will be useful for the computation at numerous investigation sites because geotechnical data for the conventional layer based modeling is not necessary.

Acknowledgments

This study is financially supported by Japan Society for the Promotion of Science (JSPS) for Grants-in-Aid for Scientific Research (KAKENHI) with the Grant Number of 23246086.

References

Cabinet Office, Government of Japan. *Investigation Committee of Nankai Trough Earthquake*. 2012. (in Japanese)

Ishikawa H, Uzuoka R, Yoshida N. Modeling Characteristics of liquefaction at the Tokushima plains. *Proc. of the 48th Japan National Conference on Geotechnical Engineering*, Toyama, Japan, 257-258, 2013. (in Japanese)

Japan Road Association (JRA). *Specifications For Highway Bridges: part V earthquake-resistant design*. Maruzen Publishing Inc.: Tokyo, 2012. (in Japanese)

Mikami T, Ichii K, Uemura H, Nishina H. The model of development of strain during undrained cyclic shear loading. *Geotechnical Engineering Journal* 2012; **7** (1): 311-322. (in Japanese)

Oka F, Yashima A, Shibata T, Kato M, Uzuoka R. FEM-FDM coupled liquefaction analysis of a porous soil using an elasto-plastic model. *Applied Scientific Research* 1994; **52**: 209-245.

Oka F, Yashima A, Tateishi A, Taguchi Y, Yamashita S. A cyclic elasto-plastic constitutive model for sand considering a plastic-strain dependence of the shear modulus. *Geotechnique* 1999; **49** (5): 661-680.

Uzuoka R, Sento N, Kazama M, Yashima A, Zhang F, Oka F. Three-dimensional numerical simulation of earthquake damage to group-piles in a liquefied ground. *Soil Dynamics and Earthquake Engineering* 2007; **27** (5): 395-413.

Uzuoka R, Cubrinovski M, Sugita H, Sato M, Tokimatsu K, Sento N, Kazama M, Zhang F, Yashima A, Oka F. Prediction of pile response to lateral spreading by 3-D soil-water coupled dynamic analysis: Shaking in the direction perpendicular to ground flow. *Soil Dynamics and Earthquake Engineering* 2008; **28** (6): 436-452.

Yasuda S, Harada K, Ishikawa K, Kanemaru Y. Characteristics of liquefaction in Tokyo Bay area by the 2011 Great East Japan Earthquake. *Soils and Foundations* 2012; **52** (5): 793-810.